Traction stress analysis and modeling reveal amoeboid migration in confined spaces is accompanied by expansive forces and requires the structural integrity of the membrane-cortex interactions.

Ai Kia Yip,[§] Keng-Hwee Chiam, [§‡] * and Paul Matsudaira[‡¶]*

[§]A*STAR Bioinformatics Institute, Singapore

[‡]Mechanobiology Institute of Singapore, National University of Singapore, Singapore

[¶]Department of Biological Sciences, National University of Singapore, Singapore

*Corresponding authors:

Keng-Hwee Chiam

A*STAR Bioinformatics Institute, 30 Biopolis Street, #07-01 Matrix, Singapore 138671

Phone: +65 6478-8264

E-mail: chiamkh@bii.a-star.edu.sg

Paul Matsudaira

Department of Biological Science, National University of Singapore, 14 Science Drive 4, Singapore 117543

Phone: +65 6516-2692

E-mail: dbsmpt@nus.edu.sg

Supplementary Methods and Material

Modelling of motility in confined environments

A schematic of the model is shown in Fig. S4. The cell was modeled in 2D and surrounded by an incompressible viscous fluid. The cell is enclosed by an elastic cell membrane that has a membrane tension T_m and a bending stiffness B_m. The cell membrane is uniformly adhered to an elastic actin cortex by membrane-cortex adhesions that are assumed to be Hookean with a spring constant k_{ad}. The elastic actin cortex also has a cortical tension T_c and a bending stiffness B_c. The cell cytoplasm and extracellular fluid are assumed to be incompressible and viscous with the same viscosity μ. The velocity field $\boldsymbol{u}$ and the pressure field $\boldsymbol{p}$ of the cytoplasmic fluid at any instant of time is described by the Stokes equation (S1) and the equation of continuity (S2), due to the low Reynolds number of the cytoplasm.

$$\nabla \boldsymbol{p} = \mu \nabla^2 \boldsymbol{u} + \boldsymbol{f}, \text{ and} \qquad \text{(S1)}$$

$$\nabla \cdot \boldsymbol{u} = 0. \qquad \text{(S2)}$$

$\boldsymbol{f}$ represents the body force on either the membrane ($\boldsymbol{f_m}$) or the actin cortex ($\boldsymbol{f_c}$).

The cell membrane is modelled as N discrete points whose positions are represented by $\boldsymbol{r}_m$. Similarly, the actin cortex is represented as discrete point whose positions are given by $\boldsymbol{r}_c$. The body force $\boldsymbol{f_m}$ on the membrane points result from membrane bending $\boldsymbol{f_{bm}}$, membrane tension $\boldsymbol{f_{tm}}$, and membrane-cortex adhesion $\boldsymbol{f_{ad}}$, as shown in Eq. (S3).

$$\mathbf{f}_m(\mathbf{r}_m) = \int_0^{Lm} [\mathbf{f}_{bm}(\mathbf{r}_m) + \mathbf{f}_{tm}(\mathbf{r}_m) + \mathbf{f}_{ad}(\mathbf{r}_m)]\delta(\mathbf{r} - \mathbf{r}_m) d\zeta_m \,, \qquad \text{(S3)}$$

where $\delta(\boldsymbol{r})$ is the two-dimensional Dirac delta function and L_m is the perimeter of the cell membrane. The no-slip boundary condition imposed on the Stokes equation gives the motion of the membrane at position $\boldsymbol{r}_m$ according to Eq. (S4).

$$\mathbf{u} = \frac{d\mathbf{r}_m}{dt} \qquad \text{(S4)}$$

The body force $\boldsymbol{f_c}$ on the cortex results from the cortex bending $\boldsymbol{f_{bc}}$, cortex tension $\boldsymbol{f_{tc}}$, membrane cortex adhesion $\boldsymbol{f_{ad}}$ and $\boldsymbol{f_{com}}$ which mimics the actomyosin contraction (Eq. (S5)). $\boldsymbol{f}_{com}$ is exerted on each of the membrane-cortex adhesion springs, in the direction tangent to the springs, thus giving rise to a uniform intracellular pressure that is higher than the surroundings.

$$\mathbf{f}_c(\mathbf{r}_c) = \int_0^{Lc} [\mathbf{f}_{bc}(\mathbf{r}_c) + \mathbf{f}_{tc}(\mathbf{r}_c) + \mathbf{f}_{ad}(\mathbf{r}_c) + \mathbf{f}_{com}(\mathbf{r}_c)]\delta(\mathbf{r} - \mathbf{r}_c) d\zeta_c \qquad \text{(S5)}$$

where L_c is the perimeter of the actin cortex.

The permeable actin cortex interacts with the cell membrane only via the membrane-cortex adhesion term $\boldsymbol{f_{ad}}$. By solving for the force balance on the actin cortex elements, the motion of the cortex at position $\boldsymbol{r_c}$ can be obtained by assuming a uniform cortical viscosity ν_c, i.e.,

$$\mathbf{f}_c = \nu_c \frac{d\mathbf{r}_c}{dt} \qquad \text{(S6)}$$

Initial detachment of the membrane-cortex adhesion springs results in nucleation of a bleb. In addition, the membrane-cortex adhesive springs would break if the spring energy exceeds the membrane-cortex adhesion energy (i.e. length of the spring is greater than a critical length l_c). To account for retraction, a second imaginary cortical element termed the diffusive cortex element is introduced. These diffusive cortical elements exist only when a region of the membrane is detached from the cortex. Upon breakage of membrane-cortex adhesive springs, these elements would move towards the bleb membrane with a speed V_c. In reality, these diffusive cortical elements represent the actin monomers which reform the cortex underneath the bleb membrane during bleb retraction. Once the diffusive cortex elements are within a distance D_{equil} from the membrane, membrane-cortex adhesive springs that are previously broken will be reattached.

Boundary integral method with regularized Stokeslets is used to solve Eq. (S1) - (S3), and (S5) for the fluid velocity field $\boldsymbol{u}$. In order to remove the singularity in the solutions of the Stokes equation subjected to point forces, we assumed that the body force $\boldsymbol{f}(\boldsymbol{r_i})$ at each discretized point spread over a small blob of radius ε.

$$\mathbf{f}_{reg}(\mathbf{r}) = \mathbf{f}(\mathbf{r}_i)\phi_c(\mathbf{r} - \mathbf{r}_i), \qquad \text{(S7)}$$

where $\phi_c(|\mathbf{r}|) = \dfrac{2\varepsilon^4}{\pi(|\mathbf{r}|^2 + \varepsilon^2)^3}$.

The membrane markers positions $\boldsymbol{r_m}$ and cortical markers positions $\boldsymbol{r_c}$ can then be updated according to Eq. (S4) and Eq. (S6) following the forward Euler method with a time step δt.

At the beginning of the simulation, the cell membrane and cortex were assumed to be cylindrical in shape. The system was allowed to equilibrate for a time period equivalent to 2 min (T_1) in real time, after which a bleb formation event was initiated by ablating 15 out of the 200 (N) discrete membrane-cortex adhesion points at one end of the cell. The simulation was then allowed to run for a further time period equivalent to 2.5 min (T_2) in real time. We also assumed that the cell does not adhere to the walls when confined between two rigid walls. The interaction between the cell and the walls is therefore purely hydro-dynamical. Zero velocity boundary conditions was imposed on the walls and the forces exerted by the walls on the fluid can be found.

The average cell migration speed was obtained by taking the net displacement of the cell's center of mass, divided by the time taken (2.5 min). The intracellular pressure was defined as the cytoplasmic fluid pressure prior to any blebbing events. All the physical and numerical parameters of the computational model are listed in Table S1 and S2.

Measurement of Young's moduli of polyacrylamide gels

The Young's moduli of the polyacrylamide gels were measured using an atomic force microscope (AFM) to indent the gels. The spherical tip of the AFM cantilever was slowly pushed into the surface of the gels by the piezoelectric stage and the position of the piezoelectric stage is denoted by Z_p, where $Z_p = 0$ at the surface of the gel. The deflection of the tip (Z_c) can be determined by the displacement of the position sensitive photo-detector

signal (V_{PSPD}). For a small deflection of the cantilever, we can assume a linear relationship where

$$Z_c = s \cdot V_{PSPD}. \qquad \text{(S8)}$$

The value of s was first obtained by pushing the AFM tip on a hard surface (glass) where $Z_p = Z_c$. The slope of a linear fit of Z_p vs V_{PSPD} curve obtained from the AFM will give us the value of s. On the other hand, on a soft surface, the AFM tip may indent into the substrate and the indentation depth δ is given by $\delta = Z_p - Z_c$. The force (F) which the tip exert on the surface can be obtained from the deflection of the tip, where $F = kZ_c$ and k represents the stiffness of the AFM cantilever as specified by the tip manufacturer.

A Hertzian model was used to obtain the Young's moduli (E) of the gels, where

$$F = \frac{4E}{3(1-\nu^2)} D^{\frac{1}{2}} \delta^{\frac{3}{2}} \qquad \text{(S9)}$$

D represents the diameter of the spherical tip specified by the tip manufacturer and ν is the Poisson's ratio of the gel. The Young's moduli of the gels can thus be obtained from the slope of the curves of F vs $\delta^{3/2}$. Measurements were conducted at several points on the gel and an averaged value was obtained as the Young's moduli of the gel (Table S3).

Supplementary Movies

Movie S1. A differentiated HL60 cell migrating in between two pieces of Pluronic-coated polyacrylamide substrates, of Young's modulus 1.25 kPa (DIC image, *far left*). Cell nuclei were stained with Hoechst (*middle left panel*, *blue*) and cells were transfected with Lifeact-GFP (*middle right panel*, *green*), which labels the F-actin. The three channels are overlaid in the *far right panel*. The number on the top of the images indicates the time in hour: minute: second.

Movie S2. A differentiated HL60 cell migrating in between two pieces of fibronectin-coated polyacrylamide substrates (100 µg/ml fibronectin), of Young's modulus 1.25 kPa (DIC image, *far left*). Cell nuclei were stained with Hoechst (*middle left panel*, *blue*) and cells were transfected with Lifeact-GFP (*middle right panel*, *green*), which labels the F-actin. The three channels are overlaid in the *far right panel*. The number on the top of the images indicates the time in hour: minute: second.

Movie S3. DIC image of a differentiated HL60 cell migrating in between two pieces of pluronic-coated polyacrylamide gels of stiffness 1.25 kPa and separated by a gap size of 2 µm.

Movie S4. DIC image of a differentiated HL60 cell migrating in between two pieces of pluronic-coated polyacrylamide gels of stiffness 1.25 kPa and separated by a gap size of 6 µm.

Movie S5. DIC image of a differentiated HL60 cell on a single piece of pluronic-coated polyacrylamide gel of stiffness 1.25 kPa (unconfined conditions).

Supporting Figures

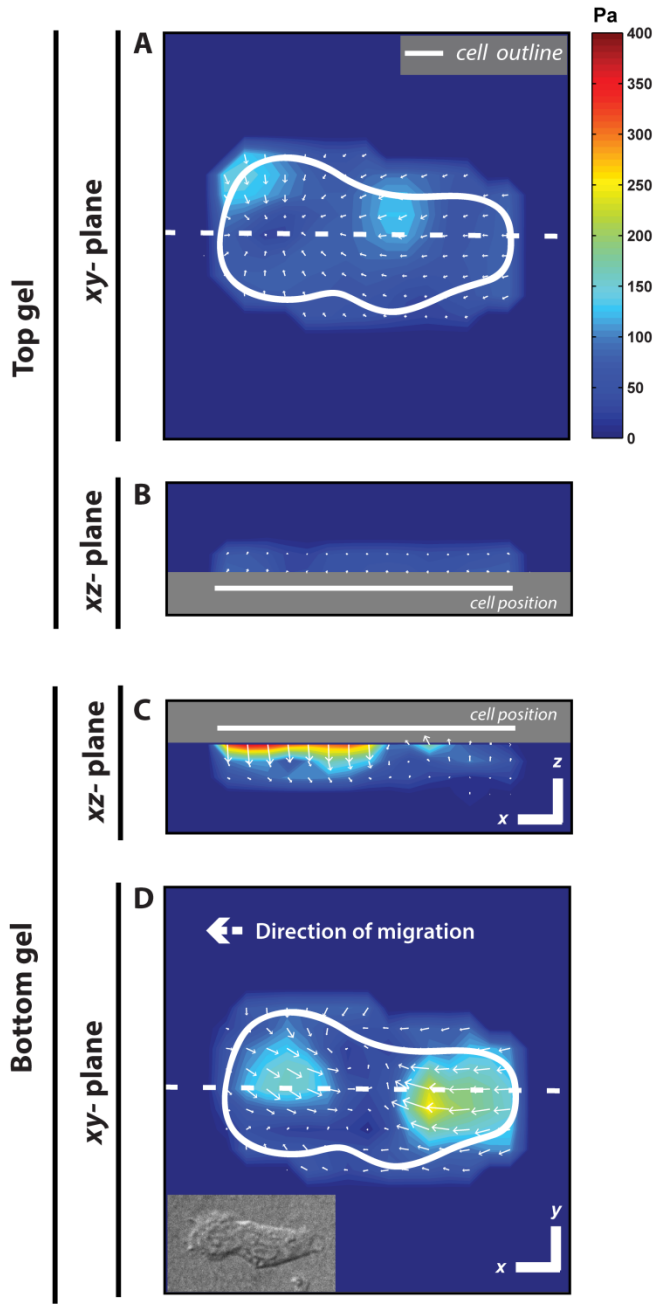

FIGURE S1. 3D traction stress measurements for a mesenchymal dHL60 cell initially plated on the bottom gel and confined between two fibronectin-coated gels, with gap size of 2 μm. *xy*-stress map of the top gel (*A*) and bottom gel (*D*) in the *xy*-plane immediately above and below the cell. Corresponding *xz*-stress map at the planes denoted by the dashed lines are shown in (*B* and *C*). Dashed arrows denote the direction of cell migration. The cell position is indicated by the white solid lines in *xy*-stress and the *xz*-stress maps. Scale bars represent 5 μm in the *x*, *y* and *z* directions. Inset in (*D*) is the DIC image of the corresponding cell.

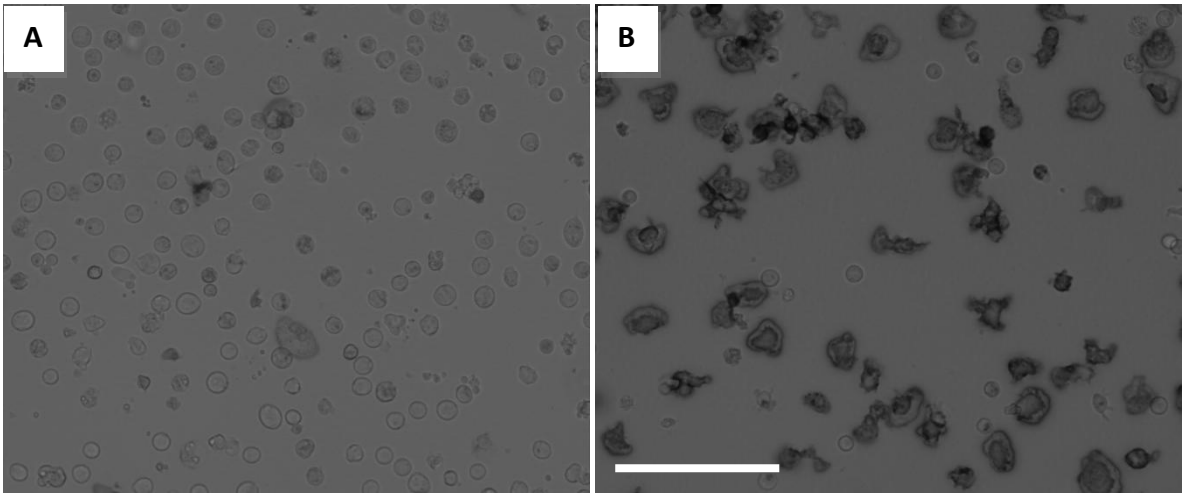

FIGURE S2. Transmitted light image of HL60 after adding 0.1% NBT. Briefly, cells were incubated in culture medium containing 0.1% NBT dissolved in PBS containing 200 ng/ml of freshly diluted 12-O-tetradecanoylphorbol-13-acetate for 40 min at 37°C. The cells were then observed under light microscope. Cells which had differentiated to neutrophils will have their nuclei stained blue. (*A*) Undifferentiated HL60: nuclei were not stained by NBT. (*B*) HL60 after incubating 6 days with 1.3% DMSO: differentiated cells' nuclei were stained blue. Scale bar represent 100 µm.

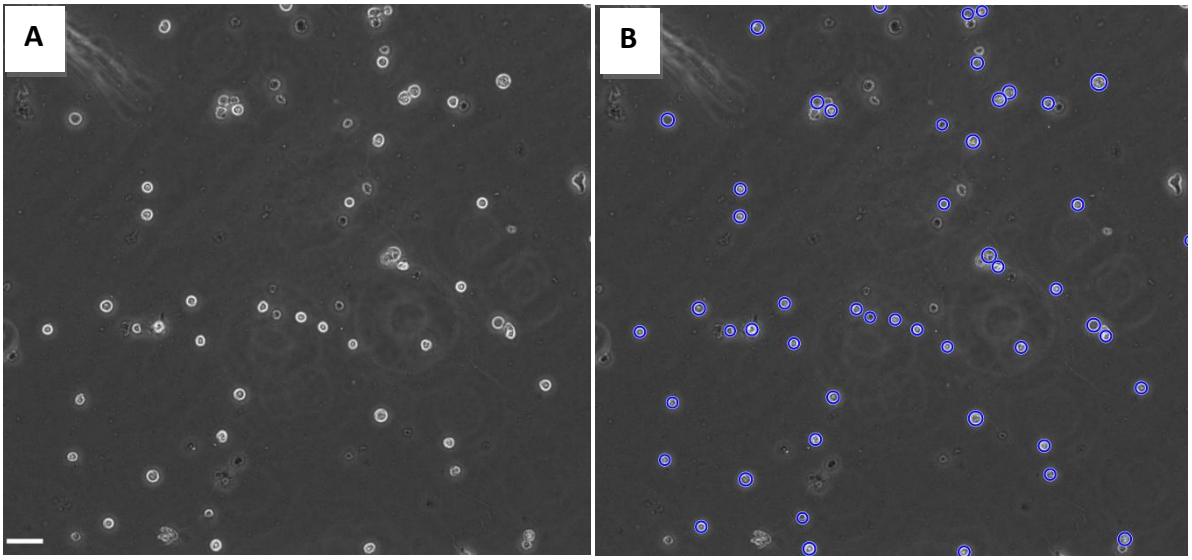

FIGURE S3. Determination of dHL60 cell diameter. (A) Phase contrast images of the dHL60 cells in suspension was obtained using the Nikon BioStation IM-Q (Nikon Instruments) at 10x magnification. Scale bar represents 50 µm. (B) Circles were fitted to the cells (blue circles) and the diameters of the circles were determined to obtain an estimate of dHL60 cell diameter.

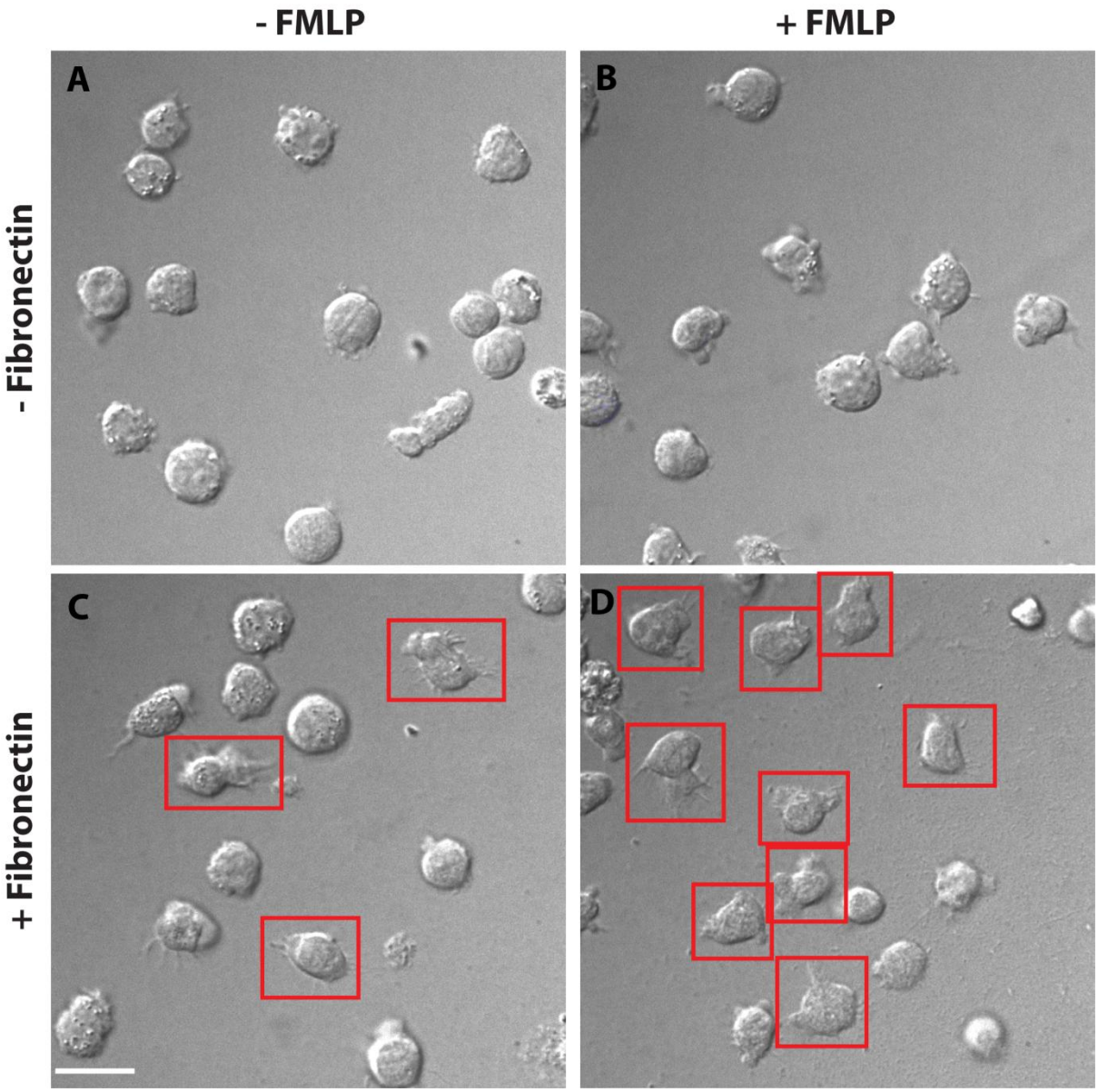

FIGURE S4. DIC image of dHL60 cell morphology with and without an uniform concentration of chemoattractant (100nM final concentration of FMLP). (*A*-*B*) Unconfined cells on Pluronic-coated (-*Fibronectin*) 1.25 kPa gels do not adhere to the substrate or form lamelipodia-/filopodia-like structures in the absence (*A*) or presence (*B*) of FMLP stimulation. (*C*-*D*) In contrast, unconfined cells on fibronectin-coated (+*Fibronectin*) 1.25 kPa gels adhere to the substrate to form lamellipodia-/filopodia-like structures (*red boxes*). A larger proportion of the cells form lamellipodia-/filopodia-like structures in the presence of FMLP stimulation (*D*). Scale bar represents 20 μm.

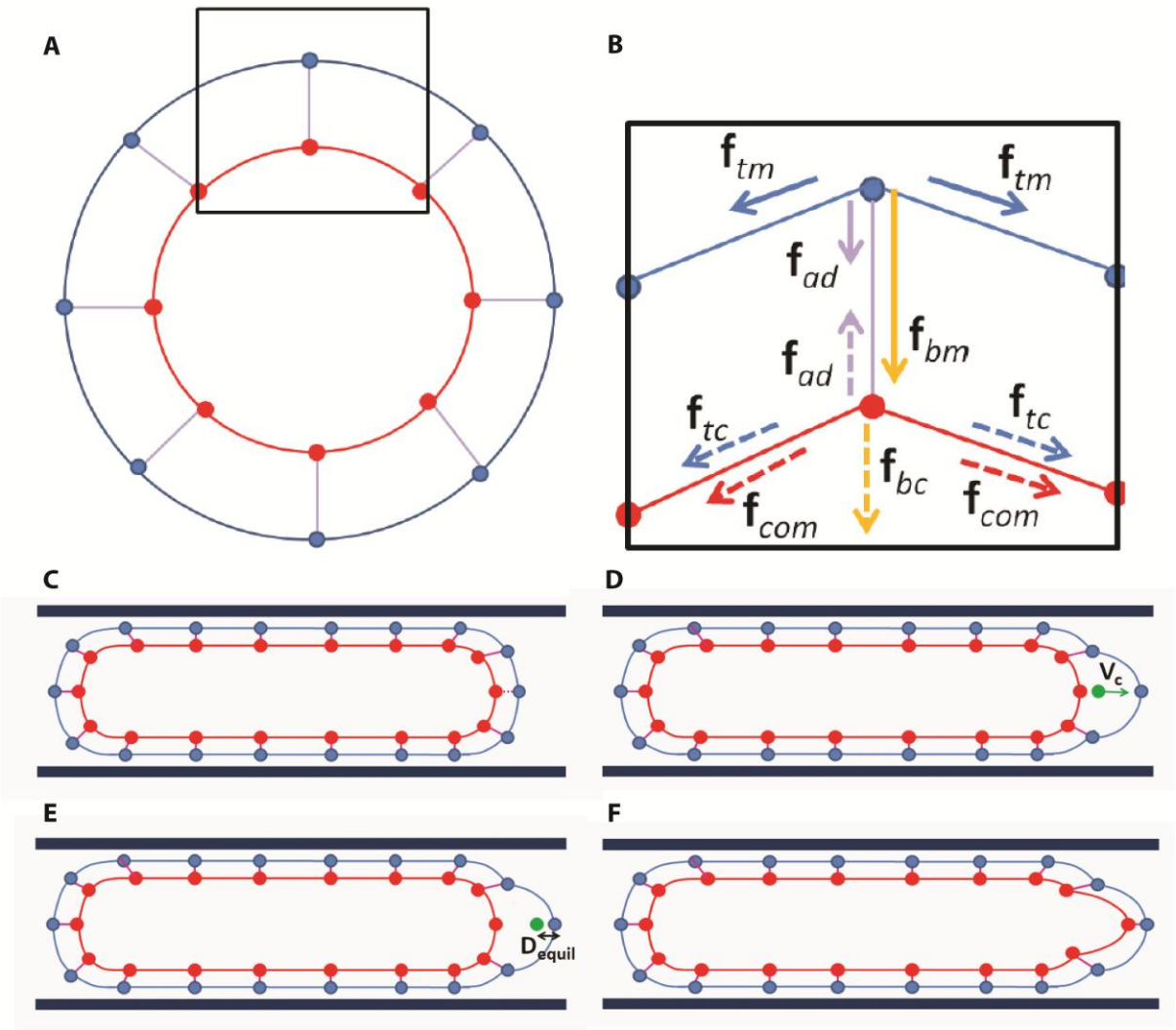

FIGURE S5. Schematic illustrations of model. (*A*) A cell is made up of the cell membrane (*blue*) and the actin cortex (*red*), connected to each other via membrane-cortex springs (*purple*). (*B*) Detailed drawing of boxed region in (*A*), with the forces acting on each point shown. (*C*) A local rupture of membrane-cortex bond (*dashed magenta line*) causes a drop in local pressure at that point. (*D*) Fluid flows into the region, down a pressure gradient, to initiate bleb formation. As fluid flows into the bleb, the free actin cortex elements (*green*) are moved into the bleb with a speed V_c. (*E*) Once the actin cortex elements are within a distance of D_{equil} from the membrane, the connections between the cortex and the membrane will reform. (*F*) This cause a retraction of the bleb and the cells' centre of mass will move. Black lines in (*C*) – (*F*) represents the rigid walls of the channel.

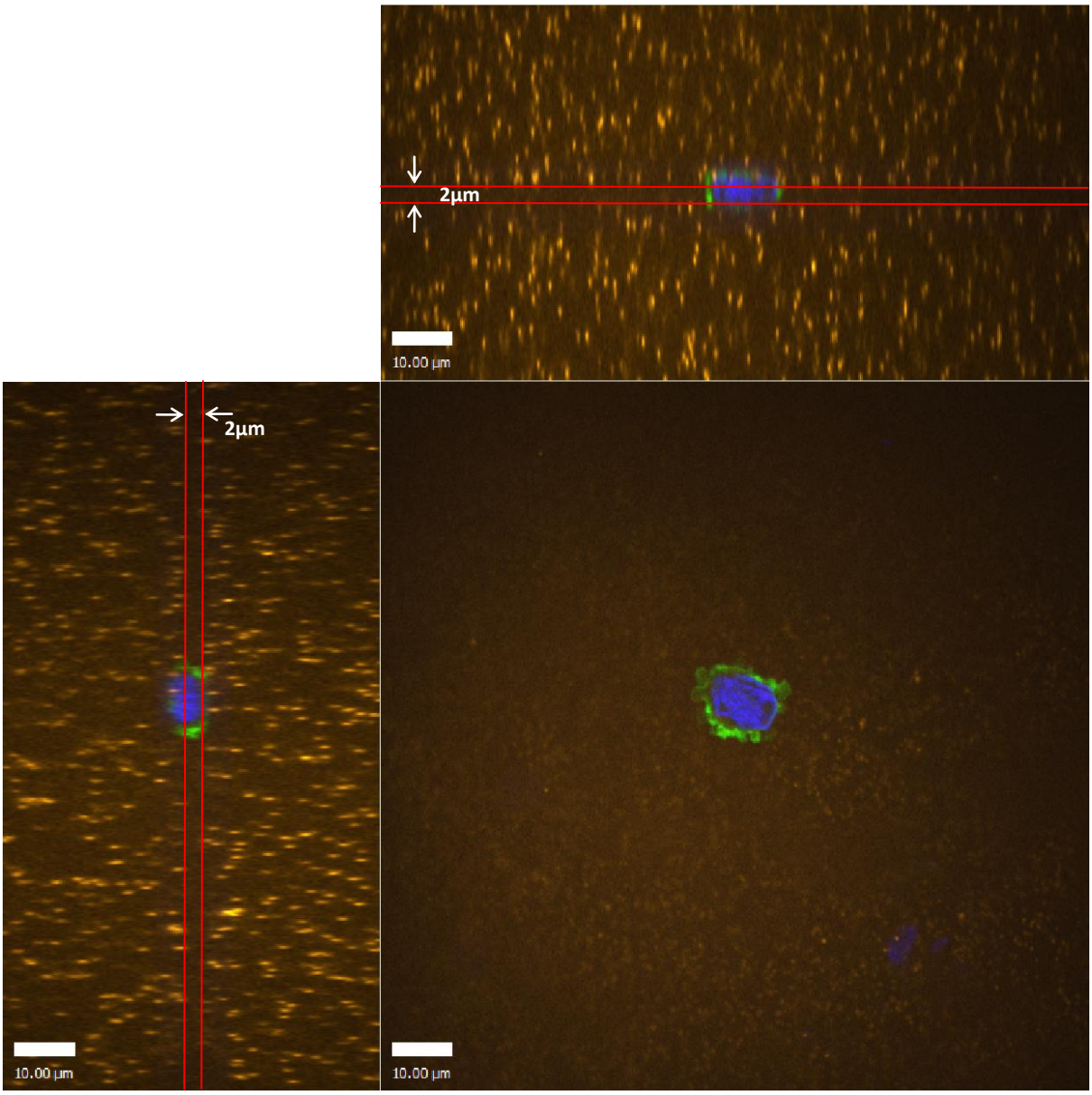

Figure S6. A dHL60 cell migrating in between two pieces of Pluronic-coated polyacrylamide substrates (with fluorescent beads embedded, *orange*), of Young's modulus 1.25 kPa and gap size of 2 µm. Red lines indicate the surfaces of the top and bottom gels. Cell nucleus was stained with Hoechst (*blue*) and the cell was transfected with Lifeact-GFP (*green*), which labels the F-actin. This figure shows that the spacing between the 2 gels are maintained at approximately the same spacing in the vicinity of the cell (at least 4 cell diameters away).

Supporting Tables

TABLE S1. Physical parameters and their corresponding values used in the computational model.

Symbol	Description	Value
r_m0	rounded cell diameter	25 μm
T_m	membrane tension	2×10^{-6} N m^{-1}
B_m	membrane bending rigidity	2×10^{-9} J
T_c	cortical tension	4×10^{-5} N m^{-1}
B_c	cortical bending rigidity	1×10^{-18} J
E_{ad}	membrane-cortex adhesion energy	0.5×10^{-6} - 8×10^{-6} N m^{-1}
k_{ad}	membrane-cortex spring constant	1×10^{6} - 16×10^{6} N m^{-3}
l_c	maximum length of membrane-cortex adhesive molecule	1 μm
f_{com}	pre-stress of the actin cortex	10 - 50 N m^{-2}
μ	cytoplasmic and extracellular fluid viscosity	1.2 Pa s
υ_c	cortical viscosity	12 kg m^{-2} s^{-1}
V_c	actin monomer diffusive speed	10 μm min^{-1}
D_{equil}	critical distance of actin cortex reformation	0.01 μm

TABLE S2. Numerical parameters and their corresponding values used in the computational model.

Symbol	Description	Value
N	number of discretized membrane and cortical elements	200
ε	blob function width of regularized force	2 μm
δt	time step	2×10^{-5} min
T_1	relaxation time	$\geq$ 2.0 min
T_2	simulation time	2.5 min

TABLE S3. Concentration of acrylamide and bisacrylamide and the corresponding Young's modulus of the gel measured by atomic force microscopy.

% Acrylamide	**% Bisacrylamide**	**Young's modulus (mean ± standard error)**	**n**
5	0.05	1.25 ± 0.016 kPa	14
8	0.1	6.19 ± 0.053 kPa	12
8	0.2	16.6 ± 0.13 kPa	7